08

Lasing in the InGaN/GaN/AlGaN disk microstructures on silicon

© E.I. Moiseev[1], S.D. Komarov[1], K.A. Ivanov[1], A.F. Tsatsul'nikov[2], E.V. Lutsenko[3], A.G. Voinilovich[3], A.V. Sakharov[2,4], D.S. Arteev[2,4], A.E. Nikolaev[4], E.E. Zavarin[2,4], D.A. Masyutin[1], A.A. Pivovarova[4], N.D. Ilyinskaya[4], I.P. Smirnova[4], L.K. Markov[4], A.E. Zhukov[1], N.V. Kryzhanovskaya[1]

[1] HSE University, St. Petersburg, Russia
[2] Submicron Heterostructures for Microelectronics, Research & Engineering Center, RAS, Saint-Petersburg, Russia
[3] Stepanov Institute of Physics, Belarusian Academy of Sciences, Minsk, Belarus
[4] Ioffe Institute, St. Petersburg, Russia
E-mail: emoiseev@hse.ru

Received February 26, 2025
Revised February 12, 2025
Accepted March 5, 2025

Microdisk lasers have been developed by using the InGaN/GaN semiconductor structure on Si substrate. Room-temperature lasing has been demonstrated in microlasers $5-8\,\mu$m in diameter operating under optical pumping in the pulsed regime on whispering gallery modes. The paper demonstrates a lasing wavelength shift from 406 to 425 nm due to a decrease in optical loss with increasing laser diameter within the gain band of the active region based on InGaN/GaN quantum wells.

Keywords: disk cavity, III-N microlaser, whispering gallery modes, silicon microlaser.

DOI: 10.61011/TPL.2025.06.61288.20298

Growing interest in creating III-N microlasers on silicon is caused by the possibility of using them as built-in light sources in silicon photonics devices [1]. When disk or ring cavities are used, lasers with a small occupied area, diameter of several micrometers (microlasers) and low lasing threshold may be constructed due to a high quality factor of the whispering gallery modes (WGM) arising because of the cavity axial symmetry [2,3]. In addition, the microdisk laser can directly and efficiently transmit radiation into the coupled waveguide, which provides great advantages in developing integrated optical devices [4]. Currently, strip-geometry lasers with InGaN/GaN quantum wells are being grown either on high-cost GaN substrates [5] or on sapphire or SiC substrates. The use of Si substrates allows realizing advantages in terms of the wafer cost, size, crystalline quality, etc. The laser effect on the GaN epitaxial layers and InGaN/GaN quantum wells grown on silicon substrates was for the first time revealed in [6,7]. When InGaN/GaN structures are grown on Si, control of defects and stresses in the layers is extremely important [8]. The task of the epitaxial GaN layer formation on the Si substrate may be solved by using multilayer buffer layers with a stepwise decrease in the $AlN/Al_xGa_{1-x}N$ composition between Si and GaN [9,10]. Another no less important issue is associated with the need to reduce the losses caused by optical mode leakage into the absorbing substrate (creation of efficient optical confinement in the direction of the structure growth) and to ensure a sufficient optical mode overlap with the active region based on InGaN/GaN quantum wells (Γ-factor) [11]. The conventional solution to this problem is formation during the structure growth of additional buffer layers ensuring optical confinement due to contrast in refractive indices. However, this approach is low-efficient in the nitride-material system because of a small difference in refractive indices and significant lattice mismatch. The most common method for reducing optical losses in the substrates for disk III-N microlasers is removal of the „sacrificial" layer and creation of a significant refractive index contrast at the semiconductor/air interface. Such a selective removal of material is typically realized by photoelectrochemical etching in structures on sapphire [12] and by selective etching of silicon in structures on silicon [13,14]. Both these methods are quite complex to implement, and the size of supports under the microcavities is hardly controllable; this affects the uniformity, quality and reproducibility of such microlasers. In this study, the III-N disk microlasers on silicon were constructed based on an approach involving a stepped buffer which efficiently acts as a lower waveguide plate and provides good field localization in the active region. Room-temperature lasing was obtained in microlasers $5-8\,\mu$m in diameter operating under pulsed optical pumping.

The epitaxial heterostructure was grown by gas-phase epitaxy from metalorganic compounds on the (111) silicon substrate (setup Dragon-125 with a horizontal inductively heated reactor). The growth rate was measured by multi-beam laser reflectometry; the surface curvature was controlled by laser deflectometry. Trimethylgallium, trimethylaluminum, trimethylindium and ammonia were used as precursors, hydrogen and nitrogen served as carrier gases. The process of growing the epitaxial structure on silicon started from depositing an AlN layer to prevent the gallium-silicon interaction with formation of eutectic (the so-called meltback etching). After that, buffer layers were grown with

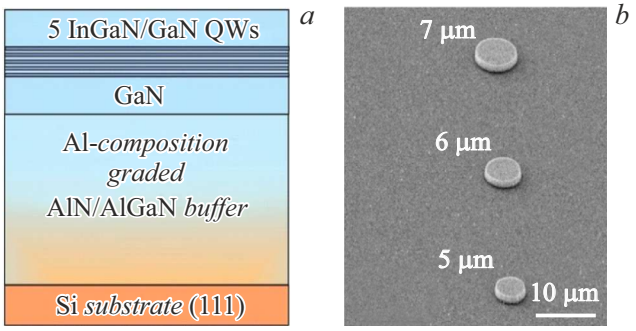

Figure 1. Schematic representation of the sample layers (*a*) and SEM image of a structure fragment with created microlasers 5, 6 and 7 μm in diameter (*b*).

a stepwise decrease in the AlN/$Al_xGa_{1-x}N$ composition. This ensures compensation of mechanical stresses arising during cooling the structure after epitaxial growth, as well as achievement of dislocation density of not higher than 10^9 cm^{-2} [15]. The grown structure contains a 200 nm thick AlN layer, combination of variable-composition AlGaN buffer layers 770 nm in total thickness, 200 nm thick GaN waveguide layer, five 2 nm thick $In_{0.1}Ga_{0.9}N$/GaN quantum wells separated by 8 nm thick GaN layers, and 200 nm thick GaN cap layer. The synthesized epitaxial heterostructure is schematically represented in Fig. 1, *a*.

Cavities 5–8 μm in diameter were created using plasma-chemical etching through a Ni mask. Etching was performed in chlorine-containing plasma in a mixture of gases (Cl_2/BCl_3) at the flow ratio of 3 : 2 and operating pressure of 5 mTorr, power of the inductively coupled plasma source $P_{ICP} = 500$ W, and power of the diode plasma source $P_{RIE} = 50$ W. The gas ratio was selected based on the necessity of obtaining a mesa wall which would be vertical and smooth simultaneously. To fabricate the metal mask, the „explosive“ photolithography technique was used because it provides almost vertical side wall, which is crucial for the etching method applied here. The metal mask was formed by successive thermal evaporation and magnetron sputtering of nickel to the thickness of about 350 nm; thickness was measured with stylus profilometer Bruker DektakXT. The nickel mask was removed by liquid etching in a solution based on sulfuric acid and hydrogen peroxide. In this case, no destruction of the structure's semiconductor layers and silicon substrate takes place. Fig. 1, *b* presents a SEM image of a fragment of the created array of microlasers 5, 6 and 7 μm in diameter. Optical pumping of microdisks was performed with a pulsed laser with an acousto-optic quality factor modulator ($\lambda = 355$ nm, pulse duration 9 ns, frequency 10 kHz). The laser beam was focused onto a single microcavity by using a Thorlabs LMU-5X-NUV objective (NA 0.12). The microlaser radiation was collected with microlens Mitutoyo Plan Apo NUV 50X (NA 0.42). The studies were performed at room temperature. The microlaser emission spectra were measured with monochromator ANDOR (Shamrock 500i) and cooled silicon multichannel detector (DU401 BVF).

To confirm the sufficiency of optical confinement from the side of substrate and to estimate the laser mode quality factor and Γ factor, field profiles and WGM natural frequencies [16] of the disk cavity 6 μm in diameter were calculated by the finite element method in the wavelength range of 400 to 430 nm. To account for the vertical optical confinement in the waveguide, there was used a quasi-3D model, i. e. a 2D cross-section geometry involving rotational symmetry with respect to the disk axis. The model included the wavelength dependence of the $Al_xGa_{1-x}N$ [17] and $In_xGa_{1-x}N$ [18] refractive indices. In modeling, a set of first-radial-order eigenmodes was obtained. Fig. 2, *a* shows the electric field modulus distribution for one of the first-

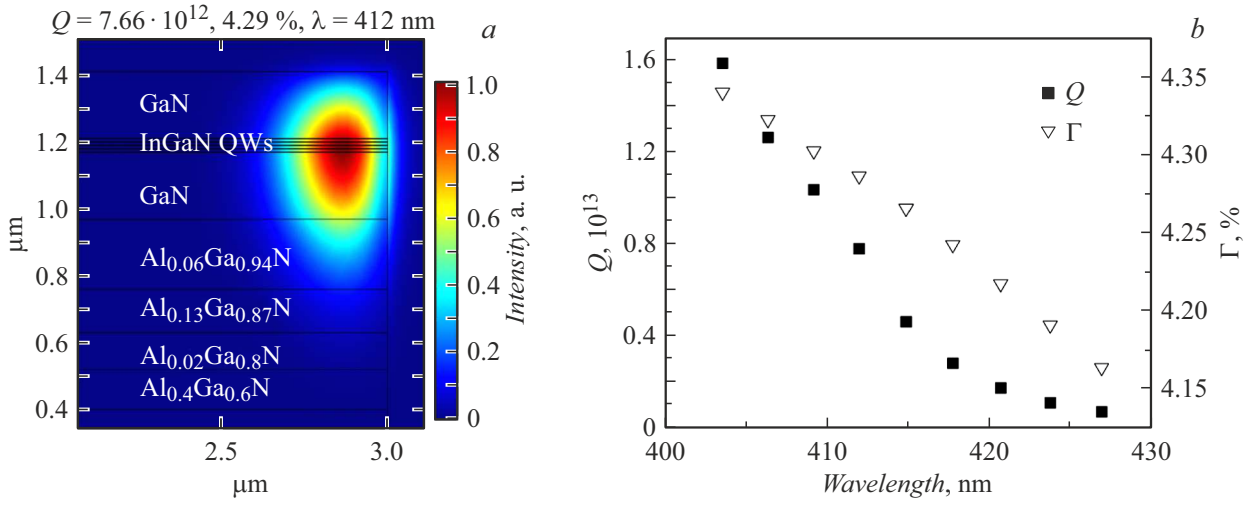

Figure 2. *a* — case distribution of the first-radial-order WGM field in the cross-section passing through the axis of disk 6 μm dia (color scale units); *b* —- spectrum of quality factors Q (squares) and Γ factors (triangles) of the first-radial-order eigenmodes in the wavelength range of 400–430 nm. The colored figure is given in the electronic version of the article.

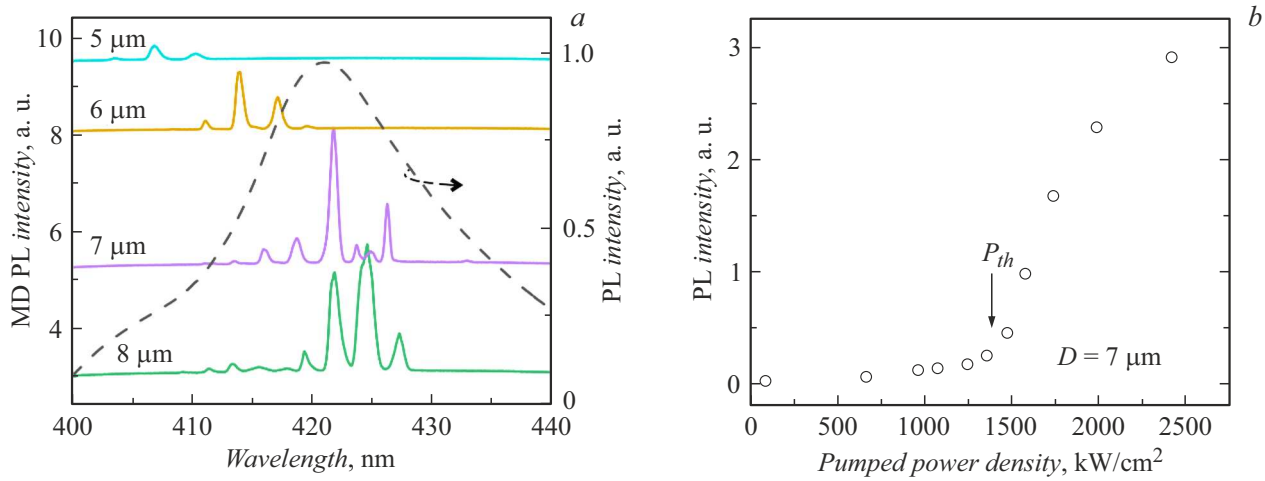

Figure 3. Room-temperature lasing spectra (left ordinate axis) for lasers 5–8 μm dia at pump power $P \sim 2P_{th}$ (spectra are shifted along the ordinate axis) and spontaneous emission spectrum of the heterostructure's $In_{0.1}Ga_{0.9}N/GaN$ quantum wells (right ordinate axis) at the pump power density of $\sim 70\,kW/cm^2$ (*a*); dependence of the 422 nm resonance line intensity on the optical pump power density for the microlaser 7 μm dia (*b*).

radial-order modes. It is evident that, despite the low contrast between adjacent layers, the proposed sequence of buffer AlGaN layers plays quite efficiently the role of the lower waveguide plate and ensures good field localization in the active region. Due to this, symmetric arrangement of quantum wells in the waveguide layer provides a sufficiently high optical confinement factor ranging from 4.15 to 4.35 %. Fig. 2, *b* presents the spectrum of eigenmodes, their quality factors and optical confinement factors. Quality factor was calculated as the ratio of the natural frequency real part to imaginary part; it depends on the field leakage through the structure boundaries (radiation losses) and absorption in the substrate. One can see that Q exceeds 10^{12} in the entire range, which indicates insignificance of losses. Thus, the obtained high values of the Γ factor and quality factor evidence the possibility of obtaining low lasing thresholds in the structure with the used layer design. The calculations give the upper estimate of quality factor, while its actual value is determined by the radiation scattering from surface roughness, absorption in the heterostructure's III-N layers and other losses that are not taken into account in modeling and may have a decisive effect on the lasing threshold.

The structure's photoluminescence spectrum measured at the optical pump power density of $70\,kW/cm^2$ exhibits a broad (FWHM of ~ 20 nm) emission line with the maximum near 422 nm corresponding to spontaneous recombination in InGaN/GaN quantum wells (Fig. 3, *a*). As the optical pump power increases, narrow lines appear in the microlasersśpectra; the most intense of them transit to the lasing mode (Fig. 3, *a*), which is confirmed by the threshold in the line intensity dependence on pump power density. A case of such a dependence is shown in Fig. 3, *b* for the microlaser 7 μm in diameter whose threshold power density appeared to be $\sim 1400\,kW/cm^2$.

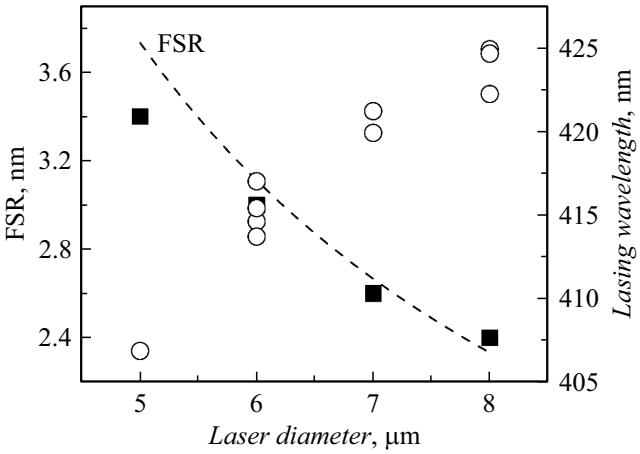

Figure 4. Experimental (squares) and calculated (dashed line) FSR dependences, and dependence of lasing wavelength spectral position (circles) on the cavity diameter.

The spectral distance between the neighboring resonance lines in the laser spectra (free spectral range, FSR) increases with decreasing cavity diameter (Fig. 4). FSR for optical whispering gallery modes is estimated as

$$\mathrm{FSR} \approx \frac{\lambda_0^2}{\pi D(n - \lambda_0 \frac{dn}{d\lambda})},$$

where λ_0 is the resonance wavelength, λ is the wavelength, D is the cavity diameter, n is the waveguide effective refractive index. Taking into account the waveguide design used here, the GaN refractive index may be taken as the n estimate. Assuming that the GaN refractive index is 2.5 and $\lambda_0 \frac{dn}{d\lambda} = -0.5$ [17], obtain a good agreement between experimental FSRs and given dependence. As the cavity diameter decreases from 8 to 5 μm, spectral

positions of resonances shift towards shorter wavelengths from 425 to 406 nm, which indicates an increase in optical loss with decreasing diameter, while lasing wavelength shifts towards the maximum of the InGaN/GaN quantum wells gain spectrum.

Thus, optimization of the III-N/Si epitaxial structure design, as well as of the technique for disk cavity fabrication, has resulted in obtaining room-temperature lasing with optical pumping in lasers $5-8\,\mu$m in diameter; the lasing wavelength is tunable within the gain band of active region based on InGaN/GaN quantum wells.

Acknowledgements

Optical measurements were performed at the Unique Research Facility „Complex Optoelectronic Stand“ (HSE University, St. Petersburg).

Funding

The article was prepared in performing the study in the framework of the HSE University project „International Academic Cooperation“.

Conflict of interests

The authors declare that they have no conflict of interests.

References

[1] M. Athanasiou, R. Smith, B. Liu, T. Wang, Sci. Rep., **4**, 7250 (2014). DOI: 10.1038/srep07250
[2] M. Feng, J. Liu, Q. Sun, H. Yang, Prog. Quantum Electron., **77**, 100323 (2021). DOI: 10.1016/j.pquantelec.2021.100323
[3] W.Y. Fu, H.W. Choi, Prog. Quantum Electron., **95**, 100516 (2024). DOI: 10.1016/j.pquantelec.2024.100516
[4] F. Tabataba-Vakili, L. Doyennette, C. Brimont, T. Guillet, S. Rennesson, B. Damilano, E. Frayssinet, J.-Y. Duboz, X. Checoury, S. Sauvage, M. El Kurdi, F. Semond, B. Gayral, P. Boucaud, Sci. Rep., **9**, 18095 (2019). DOI: 10.1038/s41598-019-54416-3
[5] S. Nakamura, M. Senoh, S.-I. Nagahama, N. Iwasa, T. Yamada, T. Matsushita, H. Kiyoku, Y. Sugimoto, T. Kozaki, H. Umemoto, Jpn. J. Appl. Phys., **37**, L309 (1998). DOI: 10.1143/JJAP.37.L309
[6] G.P. Yablonskii, E.V. Lutsenko, V.N. Pavlovskii, V.Z. Zubialevich, A.L. Gurskii, H. Kalisch, A. Szymakowskii, R.A. Jansen, A. Alam, Y. Dikme, B. Schineller, M. Heuken, Phys. Status Solidi A, **192**, 54 (2002). DOI: 10.1002/1521-396X(200207)192:1<54::AID-PSSA54>3.0.CO;2-2
[7] E.V. Lutsenko, V.N Pavlovskii, V.Z. Zubialevich, A.I. Stognij, A.L. Gurskii, V.A. Hryshanau, A.S. Shulenkov, G.P. Yablonskii, O. Schön, H. Protzmann, M. Lünenbürger, B. Schineller, Y. Dikme, R.H. Jansen, M. Heuken, Phys. Status Solidi C, **0** (1), 272 (2002). DOI: 10.1002/pssc.200390041
[8] A. Dadgar, A. Strittmatter, J. Bläsing, M. Poschenrieder, O. Contreras, P. Veit, T. Riemann, F. Bertram, A. Reiher, A. Krtschil, A. Diez, T. Hempel, T. Finger, A. Kasic, M. Schubert, D. Bimberg, F.A. Ponce, J. Christen, A. Krost, Phys. Status Solidi C, **0** (6), 1583 (2003). DOI: 10.1002/pssc.200303122
[9] K. Cheng, M. Leys, S. Degroote, B. Van Daele, S. Boeykens, J. Derluyn, M. Germain, G. Van Tendeloo, J. Engelen, G. Borghs, J. Electron. Mater., **35**, 592 (2006). DOI: 10.1007/s11664-006-0105-1
[10] B. Leung, J. Han, Q. Sun, Phys. Status Solidi C, **11** (3), 437 (2014). DOI: 10.1002/pssc.201300690
[11] L.Q. Zhang, D.S. Jiang, J.J. Zhu, D.G. Zhao, Z.S. Liu, S.M. Zhang, H. Yang, J. Appl. Phys., **105**, 023104 (2009). DOI: 10.1063/1.3068182
[12] T.J. Puchtler, A. Woolf, T. Zhu, D. Gachet, E.L. Hu, R.A. Oliver, ACS Photon., **1** (2), 137 (2015). DOI: 10.1021/ph500426g
[13] E.V. Lutsenko, A.V. Danilchyk, N.P. Tarasuk, V.N. Pavlovskii, A.L. Gurskii, G.P. Yablonskii, L. Rahimzadeh Khoshroo, H. Kalisch, R.H. Jansen, Y. Dikme, B. Schineller, M. Heuken, Superlat. Microstruct., **41** (5-6), 400 (2007). DOI: 10.1016/j.spmi.2007.03.021
[14] M. Athanasiou, R.M. Smith, J. Pugh, Y. Gong, M.J. Cryan, T. Wang, Sci. Rep., **1** (7), 10086 (2017). DOI: 10.1038/s41598-017-10712-4
[15] A.V. Sakharov, D.S. Arteev, E.E. Zavarin, A.E. Nikolaev, W.V. Lundin, N.D. Prasolov, M.A. Yagovkina, A.F. Tsatsulnikov, S.D. Fedotov, E.M. Sokolov, V.N. Statsenko, Materials, **12** (16), 4265 (2023). DOI: 10.3390/ma16124265
[16] M.L. Gorodetsky, *Opticheskie resonatory s gigantskoy dobrotnostýu* (Fizmatlit, M., 2011). (in Russian)
[17] N. Antoine-Vincent, F. Natali, M. Mihailovic, A. Vasson, J. Leymarie, P. Disseix, D. Byrne, F. Semond, J. Massies, J. Appl. Phys., **93** (9), 5222 (2003). DOI: 10.1063/1.1563293
[18] S.A. Kazazis, E. Papadomanolaki, E. Iliopoulos, IEEE J. Photovolt., **8** (1), 118 (2018). DOI: 10.1109/JPHOTOV.2017.2775164

Translated by EgoTranslating